Magnetocrystalline phase diagram of Tb: A triple line

A. Vl. Andrianov and O. A. Savel'eva
Department of Physics, Moscow State University, Moscow 119899, Russia

E. Bauer and Ch. Paul
Institut für Festkörperphysik, Technische Universität Wien, A-1040 Wien, Austria
(Received 19 July 2004; revised manuscript received 13 July 2005; published 14 October 2005)

Single crystalline terbium was examined employing both uniaxial and hydrostatic pressure. A temperature vs pressure phase diagram was compiled in both cases and, a three-dimensional magnetic phase diagram temperature vs crystalline lattice parameters was established employing a linear approximation. A triple line was obtained which separates paramagnetic, ferromagnetic, and helical antiferromagnetic phases. The temperature range where the helical antiferromagnetic phase exists is a nonlinear function of the strain. The complex magnetic states observed for Tb are interrelated with its band structure and Fermi surface shape.

DOI: 10.1103/PhysRevB.72.132408 PACS number(s): 75.25.+z, 75.30.Kz, 75.50.Ee, 71.18.+y

I. INTRODUCTION

Heavy rare-earth hexagonal close packed (hcp) metals are examples of solids in which fine structures of the Fermi surface (FS) directly determine the type of the magnetic structure. The various forms of magnetic order, i.e., helical, sinusoidal, cycloid, fan, etc., occur under different circumstances.[1] The characteristics common to all these complex structures is a magnetic wave vector q which is about an order of magnitude smaller than the Brillouine zone size, always directing along the hexagonal c axis.

More than 30 years ago Keeton *et al.*[2] suggested nesting features of the Fermi surface to determine the wave vector via mechanisms proposed for chromium.[3] According to this hypothesis, the magnetic wave vector q equals exactly a certain extreme diameter of the FS. This diameter was supposed to be the diameter of the so-called webbing feature in the L point of the Brillouin zone (see Refs. 4 and 5 for a detailed description). Within this approach, those rare-earth metals exhibiting webbing features in the FS order magnetically in a complex periodic structure. In contrast, rare-earth metals without webbing features in the FS order in a simple ferromagnetic structure. This concept is now commonly accepted. The discrepancy stated in Ref. 6 will be addressed separately.

Previously we pointed out that such webbing features are highly sensitive to minor elastic deformations.[7] In particular, a webbing feature can be created or eliminated by a proper variation of the crystalline lattice parameters that should be reflected by a respective change of the magnetic structure. This behavior is evident from general features of the band structure of these metals (see below). Moreover, we proposed a change of the type of magnetic ordering under proper elastic deformation due to qualitative changes of the FS shape driven by strain. When pressure is applied along the hexagonal axis, uniaxial compression enforces and uniaxial tension suppresses (up to a complete elimination) the complex periodic magnetic structure.

Later conclusions were supported by experiments[8,9] demonstrating that the type of magnetic ordering might actually be changed by elastic uniaxial tension or compression. In particular, the helical antiferromagnetic phase of Tb is completely suppressed by uniaxial tension as low as 680 bar in favor of a simple ferromagnetic phase.[9] The respective magnetic phase diagram temperature vs uniaxial tension appeared to be essentially nonlinear in tension. The temperature range where helical magnetic order occurs was found to depend on the uniaxial tension p_u according to the $\propto(p_u^*-p_u)^{1/2}$ law; the critical value p_u^* corresponds to the tension sufficient to eliminate the helical phase. The authors of Ref. 9 associated this critical tension with the supposed removal of the webbing feature under strain.

Thus, it might be fruitful to extend the study of this phenomenon using hydrostatic pressure. These two limiting cases, ultimately anisotropic uniaxial pressure on the one hand and isotropic hydrostatic pressure on the other might highlight the effect of the FS shape on magnetic ordering.

In a first approximation, the shape of the FS is dictated by the number of conduction electrons and by the geometry of the unit cell, but not by its actual size. A size dependence occurs only in higher order approximations; the reason is that the Brillouine zone volume always corresponds to the two free electrons per unit cell regardless of the true size of the zone. The geometry of the unit cell in the hcp structure, the hexahedral prism, is reduced to the c/a ratio of the crystalline lattice parameters i.e., the aspect ratio of the unit cell and the Brillouine zone. This ratio is thus a principal parameter specifying the FS shape of a given hcp metal. Variations of the unit cell size not affecting the c/a ratio should have a much smaller effect.

In terms of pressure this means that uniaxial pressure changing the c/a ratio should affect the FS shape and hence the magnetic structure most intensely, while isotropic pressure is expected to have significantly smaller effects. A combination of these techniques thus gives the opportunity to refine the effect of the crystalline lattice on the magnetic structure and to highlight the role of the FS. We will be also able to establish a three-dimensional (3D) temperature vs crystalline lattice parameters magnetic phase diagram.

II. EXPERIMENT

Single crystalline terbium was studied by means of resistivity measurements under hydrostatic pressure and suscep-

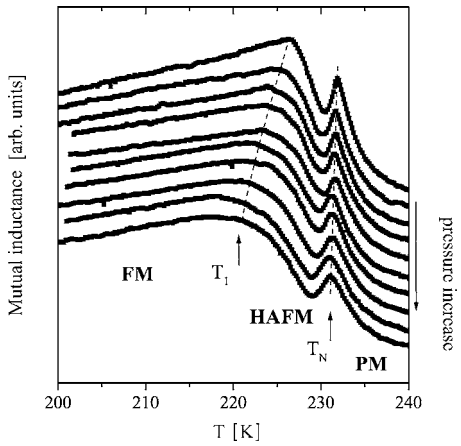

FIG. 1. Set of temperature dependencies of the mutual inductance, proportional to magnetic susceptibility $\chi(T)$, under uniaxial compression along the c axis. Curves shifted vertically for clarity, onsets omitted. Pressures from top to bottom: 0, 120, 240, 360, 470, 590, 710, 830, 940, and 1060 bar. The arrows mark T_N, the magnetic ordering temperature, and T_1, the temperature when the sample converts to the ferromagnetic phase, dashed curves are guides to eye. Abbreviations: PM, paramagnetic; HAFM, helical antiferromagnetic; and FM, simple ferromagnetic phases.

tibility measurements under uniaxial pressure. The latter experiment extends studies made in Ref. 9 under uniaxial tension. Elemental terbium was already investigated under hydrostatic pressure[11–13] and under uniaxial compression.[14] Nevertheless we carried out measurements employing both techniques on the same material used in Ref. 9 in order to obtain reliable results. All Tb samples were cut by spark erosion from the single-crystalline specimen employed by Ref. 9.

A sample with dimensions $1.50\times0.45\times0.60$ mm^3 was used for uniaxial measurements, pressure was applied along the hexagonal c axis. Technical details are given in Ref. 8. The magnetic state of the sample was examined in terms of magnetic susceptibility χ via an ac mutual inductance technique. The ac magnetic field was applied perpendicular to the c axis. Temperature dependent susceptibility $\chi(T)$ was obtained on slowly cooling the sample in N_2 atmosphere.

A piston-cylinder cell with a Teflon cap and a paraffin mixture as pressure transmitting medium served to generate hydrostatic pressure up to about 16 kbar. The absolute values of pressure were determined from the superconducting transition temperature of lead.[10] A standard dc four-probe method was employed to obtain the temperature dependent resistivity on a sample with dimensions $0.5\times0.5\times3$ mm^3, current was applied along the c axis.

III. RESULTS

The temperature dependent magnetic susceptibility $\chi(T)$ of Tb for various values of uniaxial compression is presented in Fig. 1. Distinct anomalies in $\chi(T)$ separate the paramagnetic, helical antiferromagnetic (AFM), and ferromagnetic states. The transition temperatures, marked by arrows, were obtained within an accuracy of ±0.5 K for Néel temperature

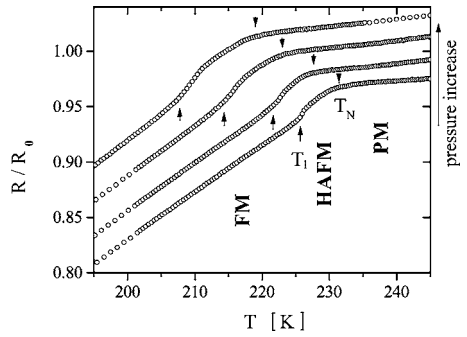

FIG. 2. Set of temperature dependencies of the resistivity measured in the basal plane under hydrostatic pressure. Curves shifted vertically for clarity. Pressures from bottom to top: 0, 4, 7.5, and 12 kbar. Arrows mark T_N, the magnetic ordering temperature, and T_1, the temperature when the sample converts to the ferromagnetic phase. Abbreviations: PM, paramagnetic; HAFM, helical antiferromagnetic; and FM, simple ferromagnetic phases.

T_N and ±1 K for T_1 where the sample converts to the simple ferromagnetic phase. To obtain T_N values, we used the common approach where this position is derived by the intersection of the two tangents drawn below and above the curvature associated with the transition. The temperature range where helical order occurs broadens with increasing pressure.

The temperature dependent resistivity $R(T)$ of Tb as a function of hydrostatic compression is shown in Fig. 2. The transitions at T_N and T_1 are accompanied by characteristic kinks, marked by arrows. The temperature range where helical order occurs also broadens under increasing hydrostatic pressure.

The dependencies of the magnetic phase transition temperatures on uniaxial pressure p_u are presented in Fig. 3(a), together with data obtained under uniaxial tension[9] (hereafter, positive pressure always means compression and negative pressure is associated with tension). The data corresponding to these two independent experiments are in good agreement, supporting the results observed in the present study. A nonlinear dependence of $T_1(p_u)$ is obvious, in contrast to the dependence of $T_N(p_u)$ that does not exhibit nonlinearity within the experimental accuracy. The dashed curve is a square-root fit. Abbreviations denote as follows: PM, paramagnetic; HAFM, helical antiferromagnetic; and FM, ferromagnetic phases. The dependencies of temperatures T_N and T_1 on hydrostatic pressure p_h, with an accuracy of ±1 K, are presented in Fig. 3(b). Note the different horizontal scales in Figs. 3(a) and 3(b).

IV. DISCUSSION

According to the above theory the transition temperatures T_N and T_1 are governed by different mechanisms. The magnetic ordering temperature T_N, proportional to the Ruderman-Kittel-Kasuya-Yosida (RKKY) exchange energy, is smoothly and almost linearly dependent on pressure. The experimental data reveal a fairly linear pressure dependence of the Néel temperature for both kinds of pressure; see the

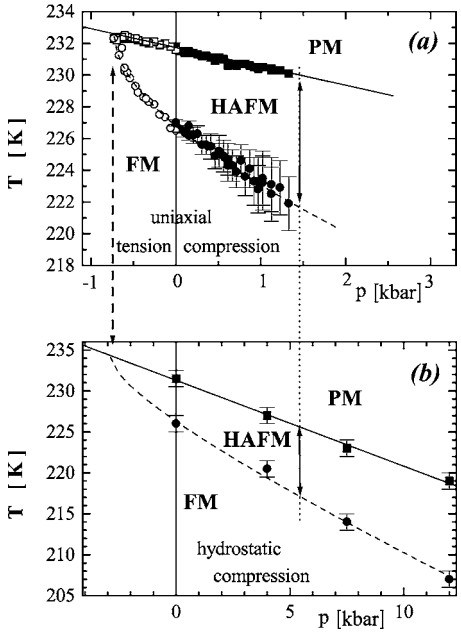

FIG. 3. Tb magnetic phase diagrams under uniaxial tension and compression (a) and hydrostatic pressure (b) note the different pressure scales. Squares, Néel temperature T_N, under tension when open and under compression when solid. Circles, temperature of conversion to the ferromagnetic phase T_1, under tension when open and under compression when solid. Abbreviations: PM, paramagnetic; HAFM, helical antiferromagnetic; FM, simple ferromagnetic phases. Vertical dotted line: arrows mark the range where helical ordering occurs, equal for (a) and (b) plots. Vertical dashed line marks magnetic triple points [suggestion for the plot (b)].

linear fits in Figs. 3(a) and 3(b). The slopes are $dT_N/dp_u = -1.23$ K/kbar and $dT_N/dp_h = -1.04$ K/kbar for uniaxial and hydrostatic pressure, respectively. The values of these coefficients obtained in Ref. 14 are −1.30 in former and −0.84 K/kbar in latter case. Inspecting Ref. 12 yields values between −0.76 and −1.07 K/kbar for dT_N/dp_h. Thus, the figures derived in the present investigation agree well with results of previous studies.

In contrast, the temperature range $\Delta T = T_N - T_1$, where helical ordering occurs, depends primarily on nesting properties of the FS. As a consequence, a nonlinear, square root-like dependence on pressure can be expected. Actually, such a square root dependence is evident for the case of uniaxial pressure [dashed curve, Fig. 3(a)]. In the case of hydrostatic pressure [Fig. 3(b)], this dependence [dashed curve, Fig. 3(b)] is also consistent with the experimental data.

Uniaxial pressure is expected to have the greatest impact on the FS and hence on the type of magnetic ordering, while isotropic hydrostatic pressure should only be of minor importance. The present experiments reveal that uniaxial pressure affects the ΔT range almost four times stronger than hydrostatic pressure. It qualitatively supports the role of the FS in magnetic ordering.

In Figs. 3(a) and 3(b) the two pressure scales are adjusted in such a manner that the temperature range ΔT is the same in both figures on the any vertical section. The example is indicated by the dashed vertical line. This presentation highlights the critical pressure values for both cases (marked by the dotted vertical line). The respective values for uniaxial and hydrostatic pressure are $p_u^* = -0.70$ kbar and $p_h^* = -2.9$ kbar, corresponding to magnetic triple points where paramagnetic, helical, and ferromagnetic phases match together.

Assuming a linear pressure dependence of the lattice parameters a and c, the pressure derivative of the lattice constants can be calculated using the elastic moduli derived for Tb:[15] $c_{11}=0.68$, $c_{12}=0.25$, $c_{13}=0.21$, and $c_{33}=0.71\times10^{12}$ dyn/cm^2. The lattice parameters of Tb at the Néel temperature and at ambient pressure are also well known:[9] $a=3.605$ Å, $c=5.695$ Å. With $D=(c_{11}+c_{12})c_{33}-2c_{13}^2$, one obtains:

	Pressure Derivative Expression	Value, 10^{-3} Å/kbar
Hydrostatic pressure	$\frac{da}{dp_h} = -\frac{c_{33}-c_{13}}{D}a$	−3.15
	$\frac{dc}{dp_h} = -\frac{c_{11}+c_{12}-2c_{13}}{D}c$	−5.08
Uniaxial pressure	$\frac{da}{dp_u} = +\frac{c_{13}}{D}a$	+1.32
	$\frac{dc}{dp_u} = -\frac{c_{11}+c_{12}}{D}c$	−9.26

The lattice parameters at the Néel temperature for each particular value of pressure can then be calculated. It allows both the phase diagrams obtained to merge into a single 3D plot "temperature vs lattice parameters." Each individual pressure dependence then provides a certain section of this plot. However, one has to keep in mind that the lattice parameters obtained are valid for the Néel temperature only, not for the magnetically ordered phases where magnetoelastic contributions to the lattice deformation cannot be estimated.

As a principal result, substituting the critical pressures p_u^* and p_h^* from Fig. 3, we obtain two triple points defining a triple line within a linear approximation: ($a=3.604$ Å, $c=5.702$ Å, $T=232.5$ K) and ($a=3.614$ Å, $c=5.710$ Å, $T=234.2$ K) for uniaxial and hydrostatic pressure, respectively. In Fig. 4 a projection of the 3D phase diagram onto the lattice parameter plane is presented. The projection of the triple line (bold-dashed) presumably separates the two feasible shapes of the FS, one with and the other one without webbing features (see the sketches in Fig. 4). The position and slope of this boundary provide valuable information on the band structure of Tb.

The range ΔT where the helical magnetic structure occurs was found to be a function of only a single parameter, i.e., any translation along this triple line does not affect the width of this range. This is, however, a trivial fact from geometry. In other words, if the 3D plot temperature vs lattice constants is viewed along the triple line obtained above, the two sections, provided by uniaxial and hydrostatic pressure, appear to coincide. This view in an axonometric projection (no perspective effects) is presented in Fig. 5. The bold lines correspond to the same fits as in Figs. 3(a) and 3(b) for both cases revealing clear coincidence.

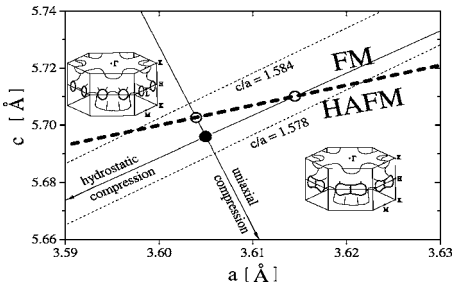

FIG. 4. Crystallomagnetic phase diagram for Tb. Solid circle, Tb under ambient pressure and Néel temperature. Straight arrows indicate the dependence of the lattice parameters on uniaxial and hydrostatic compression. Open circles correspond to magnetic triple points under uniaxial and hydrostatic compression, respectively. Dashed lines show the lines where the c/a ratio is constant as a reference (ratios indicated on the lines); the bold dashed line is a triple line, defined by two triple points, that separates the ranges of ferromagnetic (FM), and helical antiferromagnetic (HAFM) ordering. Insets: the two feasible shapes of the Fermi surface (double zone presentation), presumably separated by the triple line.

V. CONCLUSIONS

The most important result of the present study is the observation of uniaxial pressure affecting helical ordering in terbium several times more intensely than hydrostatic pressure, whereas changes in magnetic ordering temperatures are of the same order. These findings support the role of the FS geometry for the formation of a periodic magnetic structure in rare-earth metals.[15]

A crystallomagnetic phase diagram is derived for single crystalline Tb comprising a linear approximation. A triple line, where paramagnetic, helical, and ferromagnetic phases match together was drafted. This line is also expected to separate the two feasible shapes of the Fermi surface: that with webbing features responsible for magnetic nesting, and that without such a FS shape. This result provides new information on the electronic structure of Tb and allows qualitative comparison with band structure calculations. It may also be useful for studies of high stressed objects such as epitaxial films.

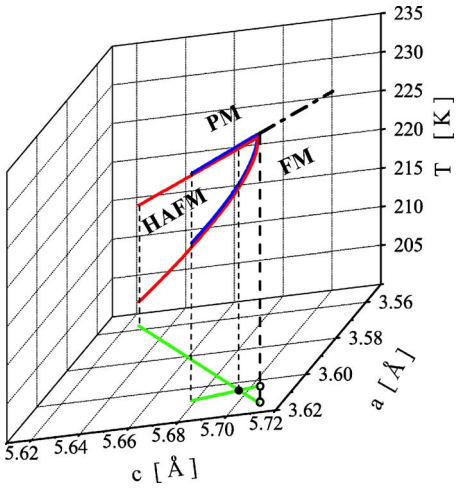

FIG. 5. (Color online) 3D crystallomagnetic phase diagram for Tb viewed along the triple line (see text). Its projection on the c-a plane is shown in Fig. 4. Solid circle, Tb under ambient pressure and Néel temperature, open circles correspond to the magnetic triple points under uniaxial and hydrostatic compression, respectively. Dashed lines mark the projections on the horizontal plane, bold dashed line marks the projection of the triple line. Abbreviations: PM, paramagnetic; HAFM, helical antiferromagnetic; FM, simple ferromagnetic phases.

ACKNOWLEDGMENTS

This work was supported by the Russian Foundation for Basic Research (Grant Nos. 01-02-02010-BNTS and 04-02-16865), by the Austrian-Russian Science program, Project No. Nr.I.2/2001, and by the Austrian FWF, Project No. P 12899. A. A. and O. S. are grateful to R. Z. Levitin and Yu. P. Gaidukov for the useful discussions.

[1] J. Jensen and A. R. Macintosh, *Rare Earth Magnetism* (Clarendon Press, Oxford, 1991).
[2] S. C. Keeton and T. L. Loucks, Phys. Rev. **168**, 672 (1968).
[3] W. M. Lomer, Proc. Phys. Soc. London **80**, 489 (1962).
[4] S. B. Dugdale, H. M. Fretwell, M. A. Alam, G. Kontrym-Sznajd, R. N. West, and S. Badrzadeh, Phys. Rev. Lett. **79**, 941 (1997).
[5] V. Thakor, J. B. Staunton, J. Poulter, S. Ostanin, B. Ginatempo, and E. Bruno, Phys. Rev. B **68**, 134412 (2003).
[6] S. J. Crowe, S. B. Dugdale, Zs. Major, M. A. Alam, J. A. Duffy, and S. B. Palmer, Europhys. Lett. **65**, 235 (2004).
[7] A. Andrianov, Sov. Phys. JETP **55**, 666 (1992); A. Andrianov, J. Magn. Magn. Mater. **140–144**, 749 (1995).
[8] A. Vl. Andrianov and O. D. Chistiakov, Phys. Rev. B **55**, 14107 (1997).
[9] A. Vl. Andrianov, D. I. Kosarev, and A. I. Beskrovnyi, Phys. Rev. B **62**, 13844 (2000).
[10] A. Eiling and J. Schilling, J. Phys. F: Met. Phys. **11**, 623 (1981).
[11] G. S. Fleming and S. H. Liu, Phys. Rev. B **2**, 164 (1970).
[12] H. Umebayashi, G. Shirane, B. C. Frazer, and W. B. Daniels, Phys. Rev. **165**, 688 (1968).
[13] S. Kawano, N. Achiwa, A. Onodera, and I. Nakai, Physica B **180–181**, 46 (1992).
[14] H. Bartolin, J. Beille, D. Bloch, P. Boutron, J. L. Feron, J. Appl. Phys. **42**, 1679 (1971).
[15] Landolt-Börnstein, New Series, Group III, vol. 11, p. 41 (Springer-Verlag, Berlin, 1979).